Light-Scattering Study of the Association Behavior of Styrene–Ethylene Oxide Block Copolymers in Aqueous Solution

Renliang Xu and Mitchell A. Winnik*

Department of Chemistry and Erindale College, University of Toronto, Toronto, Ontario, Canada M5S 1A1

F. R. Hallett

Guelph–Waterloo Program for Graduate Work in Physics and Department of Physics, University of Guelph, Guelph, Ontario, Canada N1G 2W1

Gérard Riess

Ecole Nationale Superieure de Chimie, 33 rue Werner, 68093 Mulhouse Cedex, France

Melvin D. Croucher

Xerox Research Centre of Canada, 2660 Speakman Drive, Mississauga, Ontario, Canada L5K 2L1

Received February 22, 1990; Revised Manuscript Received May 22, 1990

ABSTRACT: Static and dynamic light-scatterning studies on the micellization behavior in aqueous solution of poly(styrene–oxyethylene) diblock and poly(oxyethylene–styrene–oxyethylene) triblock copolymer are presented. Two narrowly distributed populations of particles are found in the solution. The sizes of the large particles and the small particles remain unchanged in a concentration range from 2×10^{-5} to 2×10^{-3} g/mL. The weight fraction of the large particles, however, decreases with increasing concentration, unlike in most common aggregation processes. Detailed analysis reveals that the small particles ($R_h \sim 20$ nm) are regular micelles with association number of a few hundreds, and the large particles ($R_h \sim 65$ nm) are loose micellar clusters consisting of tens of micelles. The micelle structure is core–shell type with a dense and glassy polystyrene core and a highly swollen poly(oxyethylene) shell.

Introduction

Many studies have shown that block copolymers form micelles of closed association upon dissolution into a selective solvent, which acts thermodynamically as a good solvent for one block and a precipitant for the other block.[1] Less is known about block copolymers involving water-soluble blocks. These materials have important properties that are very useful from a technological point of view, such as steric stabilizers for latex particles and as dye or pigment vehicles in printing technologies. Micelle structures are also found in natural transport systems. For example, lipoproteins carry hydrophobic cholesterol–esters in the blood serum. Micelles in aqueous solution, with hydrophilic blocks such as poly(ethylene oxide) and hydrophobic blocks having side-chain units such as poly(L-lysine) on which drugs could be attached, have potential use as drug-carrier systems.[2] Thus, micelles in aqueous solution are drawing ever-increasing attention in contemporary research.

A variety of different techniques have been used to examine the structural and colloidal properties, as well as the micellization process, of block copolymer associations. The most reliable results on micelle structure have come from light-scattering and X-ray scattering studies involving the index-matching technique: through choice of solvents isorefractive to one or the other copolymer block. The requirement is difficult to fulfill in aqueous solution, since most polymers have refractive indices much higher than that of water. The problem is compounded by the complexity of these systems, in composition, in polydispersity, and in optical and geometrical heterogeneity. Measurements give results that are averages over these various distributions, and the interpretation of these results has at times been controversial. One of the most interesting findings is that some block copolymer micelle systems, in fact, exist in two populations, i.e., a bimodal size distribution.[3–5]

These self-organizing systems have fascinated theorists. Many theoretical treatment of copolymer micelle formation, pioneered by de Gennes,[6] have been proposed in the past decade.[7–12] The objective has been to describe the colloidal properties (radius, association number) in terms of copolymer chain length and block length. The two key contributors to micelle structure are the interfacial energy of the micelle core with solvent and the conformational distortion energy of the soluble chains emanating from the core. Within the context of this core–shell model and further simplifying assumptions, the various theories seek to minimize the total Gibbs free energy by means of explicit calculation or via scaling approaches in which numerical coefficients are purposefully omitted.

In general, one finds that theories that assume a constant shell density, e.g., uniform concentration of polymer segments within the shell, independent of the distance from the micellar core, often fail to fit experimental results. The star model,[9] in which the segment concentration in the shell decreases with increasing distance from the micellar center, represents a significant improvement. However, for the scaling approaches, only trends in a series of copolymer micelle systems can be predicted; and for the explicit expressions, numerical parameters, such as the interaction parameter and the interfacial tension, are system dependent and not always available. Thus, systematic comparison between theory and experimental results are still rare.

* To whom correspondence should be addressed.

0024-9297/91/2224-0087$02.50/0

Table I
Properties of the Copolymer Samples

sample	structure	W_A[a] (PEO wt %)	M_n[a]	N_B[b] (PS)	N_A[b] (PEO)	$(dn/dc)_{calc}$,[c] mL/g	$(dn/dc)_{meas}$,[c] mL/g	cmc,[d] g/mL
23	AB	61.0	28 700	108	400	0.176	0.17	1×10^{-6}
41	AB	84.4	23 500	35	450	0.151	0.17	4×10^{-6}
19	ABA	69.0	13 100	39	102 + 102	0.165	0.18	4×10^{-6}

[a] Determined by gel-permeation chromatography for an aliquot of the first-stage polystyrene compound and by ^{1}H NMR for the purified block copolymer. [b] Number-averaged monomer units per polymer. [c] Calculated according to eq 1. [d] Critical micelle concentration; value from ref 16.

Studies of the micellization of polystyrene–poly(ethylene oxide) (PS–PEO) block copolymer, which contains hydrophilic block (PEO, denoted as A) and hydrophobic block (PS, denoted as B) sequences, in aqueous solutions have been carried out in a number of laboratories by using turbidity and viscosity measurements, a fluorescence probe technique, and high-resolution NMR.[3,13-19] An interesting feature of these micelles is that the hydrophobic polystyrene core remains glassy up to temperatures approaching the boiling point of water, which reveals a potential application of such micelles for encapsulating materials. More investigations are still needed in order to understand the micelle structure of PS–PEO block copolymer in aqueous solution. In the present study, dynamic and static light-scattering measurements are performed to study both di- (AB) and triblock (ABA) PS–PEO copolymers of different molecular weights in water. Our results show that there are two narrowly distributed populations of particles in solution. The population ratio of the two components is copolymer concentration dependent. The analysis based on a star model shows that the small particles are regular micelles and the large ones are loose micellar clusters.

Experimental Section

1. Sample Preparation. Styrene–ethylene oxide diblock (AB) and triblock (ABA) copolymers were prepared in THF by anionic polymerization.[20] They were then purified and characterized.[21] Table I shows the compositions and the molecular weights of the three samples investigated.

The dilute solutions of the copolymers were prepared by dissolving the sample into a THF–water mixture. Both HPLC-grade THF and deionized (milli-Q grade) water were distilled before use. After heating the solution for a short period of time ($\sim^1/_2$ h) with a water bath ($\sim$60 °C), THF was then removed by azeotropic distillation under reduced pressure. Gas–liquid chromatography measurements indicated that the residual THF in the sample was negligible.[16] The three stock aqueous solutions had concentrations on the order of 10^{-3} g/mL. The dilution by distilled water was made a few days later. To ensure that all our samples were in the dilute micelle solution region, but still above the critical micelle concentration (cmc), we chose the concentration range of the solutions to span 2×10^{-5} to 2×10^{-3} g/mL. The aqueous solutions were then centrifuged at 12 000 rpm ($\sim$17 000 g) using a Sorval RC2-B centrifuge for 2 h to remove foreign materials before being transferred into the light-scattering cells.

To ensure the reproducibility of the micelle solution in terms of micellar size, several preparations from the same copolymer sample were performed. Experiments were carried out over a several month period, primarily at Guelph University, with some experiments also carried out at SUNY—Stony Brook in the laboratory of Professor B. Chu. Each set of measurements employed samples prepared independently. Results of quasi-elastic light-scattering measurements were independent of sample series, equipment, or software for data analysis.

2. Refractive Index Increment. The refractive index increment of a copolymer is a linear function of its composition

$$\left(\frac{dn}{dc}\right) = W_A\left(\frac{dn}{dc}\right)_A + W_B\left(\frac{dn}{dc}\right)_B \quad (1)$$

where (dn/dc), $(dn/dc)_A$, $(dn/dc)_B$, W_A, and W_B are the refractive index increments of the copolymer and of the homopolymers A and B and the weight fractions of A and B in the copolymer, respectively. The values of $(dn/dc)_A = 0.134$ at $\lambda_0 = 632.8$ nm could be found in ref 22 and of $(dn/dc)_B = 0.241$ at $\lambda_0 = 589$ nm in ref 23 at room temperature. The calculated values for the refractive index increments of the three samples are listed in Table I. The measurements of (dn/dc) of the copolymer solutions were performed by using a KMX-16 laser differential refractometer at $\lambda_0 = 632.8$ nm. The values are also listed in Table I.

3. Light-Scattering Measurement. Two laboratory-built light-scattering spectrometers, both equipped with 50-mW He–Ne lasers that produce vertically polarized incident beams at $\lambda_0 = 632.8$ nm, were used in the present study. The cell was held in a brass thermostat block filled with refractive index matching silicone oil at room temperature. The vertically scattered beam was collected over an angular range of 20–130° for either absolute integrated intensity or photon correlation spectroscopy measurements. The details of the instrumentation at Guelph[24] and at SUNY—Stony Brook[25] have been described elsewhere.

Our data analysis presumes an equilibrium between the copolymer molecules (unimers) and the micelles (N-mers) in micelle solutions. Hence, the solution at the cmc can be considered to be the "solvent" for the micelles. Below the cmc there should be no (or a negligible amount of) micelles; above the cmc all added copolymer molecules would take the micellar form. This assumption is probably incorrect for block copolymers of finite polydispersity but is mitigated by the fact that the cmc for these samples lies at a concentration 1 order of magnitude lower than the most dilute solution from which light-scattering data can be obtained. Thus, in the dilute solution regime

$$\frac{H(C - \mathrm{cmc})}{R_{vv}} = \frac{1}{M_{w,app}}\left(1 + \frac{K^2\langle R_g^2\rangle_{z,app}}{3}\right) + 2A_2(C - \mathrm{cmc}) \quad (2)$$

with $H = (4\pi^2 n^2 (dn/dc)^2)/(N_A \lambda_0^4)$ (with N_A Avogadro's number, n the refractive index of pure solvent, and λ_0 the wavelength of light in vacuo, respectively). Here R_{vv} is the excess Rayleigh ratio. K, the scattering vector, is equal to $(4\pi n/\lambda_0)\sin(\theta/2)$. $M_{w,app}$ is the apparent weight-averaged molecular weight, $\langle R_g^2\rangle_{z,app}$, the apparent z-averaged squared radius of gyration, A_2, the second virial coefficient, and C, the total concentration in grams per milliliter. The known Rayleigh ratio of benzene was used as a calibration standard. The cmc values were determined by steady-state fluorescence spectroscopy using pyrene as a fluorescent probe.[16] Values are listed in Table I. It is important to note that since PS and PEO have very different refractive indices ($n_{PS} = 1.583$ and $n_{PEO} = 1.456$ at $\lambda_0 = 589$ nm) and the copolymers are heterogeneous in chemical composition as well as in scattering power, eq 2 yields only apparent values rather than true values of M_w and $\langle R_g^2\rangle_z$.

For copolymer micelle solutions, the apparent value of $M_{w,app}$ is related to the true value M_w in the form[26]

$$M_{w,app}\left(\frac{dn}{dc}\right)^2 = M_w\left(\frac{dn}{dc}\right)_A\left(\frac{dn}{dc}\right)_B + \left(\left(\frac{dn}{dc}\right)_A^2 - \left(\frac{dn}{dc}\right)_A\left(\frac{dn}{dc}\right)_B\right)W_A M_w^A + \left(\left(\frac{dn}{dc}\right)_B^2 - \left(\frac{dn}{dc}\right)_A\left(\frac{dn}{dc}\right)_B\right)W_B M_w^B \quad (3)$$

with M_w^A and M_w^B being the weight-averaged molecular weights of the components A and B and W_A and W_B being the weight-averaged weight fractions of A and B, respectively. If the micelles have a narrow distribution of association numbers (N), as

a first-order approximation we can rearrange eq 3 to

$$M_{w,app}\left(\frac{dn}{dc}\right)^2/N = M_n\left(\frac{dn}{dc}\right)_A\left(\frac{dn}{dc}\right)_B + \left(\left(\frac{dn}{dc}\right)_A^2 - \left(\frac{dn}{dc}\right)_A\left(\frac{dn}{dc}\right)_B\right)W_A M_n^A + \left(\left(\frac{dn}{dc}\right)_B^2 - \left(\frac{dn}{dc}\right)_A\left(\frac{dn}{dc}\right)_B\right)W_B M_n^B \quad (4)$$

The subscripts w now are replaced by n to imply the corresponding molecular weight of the copolymer molecules.

When the above values of $(dn/dc)_A$ and $(dn/dc)_B$ (assuming little wavelength dependence for $(dn/dc)_B$) and the molecular weight and the composition of our samples are used, the average numbers N and the molecular weights of the micelles can be obtained from the intercepts of the Zimm plots, even without knowing the dn/dc values of the block copolymers in water.

Compared with the molecular weight, the interpretation of the angular dependence of the scattered light intensity is much more complicated. Due to the refractive index inhomogeneity, the individual monomeric units (i.e., scattering centers) differ in their scattering power, and the angular dependence of the scattered intensity cannot be described by a conventional particle scattering function in which the scattering centers are assumed all to be identical. The apparent radius of gyration is composition, solvent, and micelle-conformation dependent. In principle a characteristic quantity analogous to the radius of gyration of homopolymers can be determined only if three (or more) different $R_{g,app}$ values are measured in three (or more) solvents with different refractive indices. In practice not only are the equations awkward but one cannot expect that the conformations of the micelles are exactly the same in all the solvents employed. The conformational variation also prevents the use of the index-matching technique, which requires adding a second solvent.

The intensity–intensity photon correlation functions were measured by a Langley Ford 1096 correlator (at Guelph) and a Brookhaven BI2030AT correlator (at Stony Brook). Since the information-retrieving procedure from the autocorrelation function was very sensitive to the signal-to-noise ratio, the criterion to accept a measured correlation function is that the measured base line, i.e., the average value of the correlation function at very long delay times, agreed with the computed base line to within ~0.1%. The general formula for the photoelectron count time correlation function in the self-beating mode has the form

$$G^{(2)}(\tau) = A(1 + \beta|g^{(1)}(\tau)|^2) = A(1 + \beta \exp(-2\bar{\Gamma}\tau)) \quad (5)$$

with $G^{(2)}(\tau)$ being the intensity–intensity autocorrelation function, β a spatial coherent coefficient for instrument beating efficiency, A the base line; $g^{(1)}(\tau)$ the normalized electric field autocorrelation function, τ the delay time, and $\bar{\Gamma}$ the average characteristic line width.

For the polydisperse system the characteristic line-width distribution ($G(\Gamma)$) has to be taken into account; thus

$$g^{(1)}(\tau) = \int G(\Gamma) \exp(-\Gamma\tau)\, d\Gamma; \quad \bar{\Gamma} = \int \Gamma G(\Gamma)\, d\Gamma \quad (6)$$

The ill-posed Laplace inversion of eq 6, from which $G(\Gamma)$ was obtained from the measured $g^{(1)}(\tau)$, was processed mainly by the Non-Negatively Least Squares (NNLS) (at Guelph and at Stony Brook) and the regularized continuous inversion of Laplace integral equation (CONTIN) algorithms (at Stony Brook).[27] The output from the two methods was very close to each other. For spherical particles, the characteristic line width, Γ, is related to the translational diffusion coefficient D_T ($=\Gamma/K^2$) provided that the internal motions are negligible. In the dilute-solution region, the concentration dependence of the translational diffusion coefficient can be expressed by a first-order expansion

$$D_T = D_0(1 + k_D C) \quad (7)$$

with D_0 and k_D being, respectively, the translational diffusion coefficient at infinite dilution and the diffusion second virial coefficient. Thus, from the analysis of the characteristic line width, Γ, the equivalent hydrodynamic radius of the particle could be obtained when the Stokes–Einstein relation is applied

$$R_h = \frac{k_B T}{6\pi\eta D_0} \quad (8)$$

where k_B, T, and η are Boltzmann constant, the absolute temperature, and the solvent viscosity, respectively.

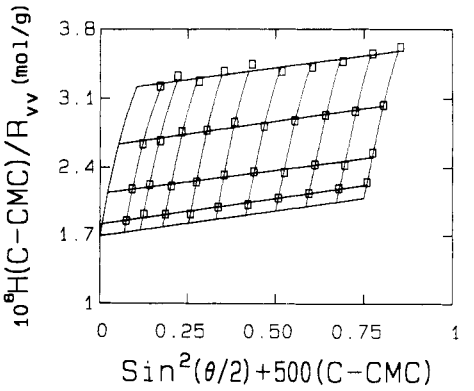

Figure 1. Zimm plot for sample no. 23.

Results and Discussion

1. Average Values of Molecular Weights, Association Numbers, and Apparent Radii of Gyration. From the concentration and angular extrapolations of the excess integrated scattered intensity of the copolymer samples in dilute aqueous solution, i.e., from the Zimm plots (for example, Figure 1), we obtained the apparent molecular weights ($M_{w,app}$). When eq 4 and the values of the refractive index increments of the corresponding homopolymers are used, the weight-averaged molecular weights (M_w) and the corresponding average association numbers (N) could be computed. The results are listed in Table II. The samples we examined here have been described in previous publications from the Riess group,[13,14] using simplified approaches in the determination of the micelle aggregation number. The trend of our results is in agreement with the conclusion of ref 13; i.e., the association degree of the micelles increases by increasing the molecular weight of the copolymer or by decreasing the PEO content. The M_w of No. 41 is not the same either as the value in ref 13 (2.4×10^6 g/mol) or as that in ref 14 (3.6×10^7 g/mol). The depolarization ratios (R_{vh}/R_{vv}) of the micelles in aqueous solutions were all very small (<1%), which identified their isotropic property. It should be noted that the value of the second virial coefficient increased with increasing of PEO content of the block copolymer and decreased with increasing the association number of the micelle.

2. Average Translational Diffusion Coefficient. Photoelectron autocorrelation function provided hydrodynamic information about the micelles in solutions. Since the measurements were performed in a space range of $KR_h < 1$ (e.g., at a scattering angle of 90°: for a particle of R_h being 50 nm, $KR_h = 0.9$), the angular dependence of the scaled characteristic line width ($\bar{\Gamma}/K^2$) should be negligible. Furthermore, for spherical particles, $\bar{\Gamma}/K^2$ should be independent of the detection angle because of the undetectable rotational motion. However, our analysis of the correlation function showed that the average values of $\bar{\Gamma}/K^2$ had a small angular dependence as shown typically in Figure 2. This is an indication either of polydispersity or of a multimodal distribution of micelles in solution. We will find it convenient to use the word "paucidispersity" to refer to the situation where the distribution of sizes comprises two (or more) very narrowly distributed population of micelles. For different particle sizes different rates of decrease of the scattering form factors would be observed when increasing the scattering angle. In particular, all populations had their scattering form factor $P(KR_h) \sim 1$ at small scattering angles, and the measured

Table II
Parameters for PS-PEO Copolymers in Aqueous Solutions

sample	$M_{w,app}$[a]	M_w[b]	N[b]	$\langle R_{g,app}^2\rangle_z^{1/2}$, nm	A_2, mol·mL/g^2	$\bar{D}_0$,[c] 10^{-8} cm^2/s	$\bar{k}_D$, cm^3/g
23	5.9×10^7	4.5×10^7	1560	36	4.9×10^{-5}	5.2	1700
41	8.8×10^6	9.0×10^6	380	37	1.3×10^{-3}	7.3	820
19	6.3×10^6	5.2×10^6	400	43	3.3×10^{-4}	9.5	480

[a] $M_{w,app}$, $\langle R_{g,app}^2\rangle_z^{1/2}$, and A_2 were obtained from static light-scattering measurements. [b] M_w and N were computed according to eqs 3 and 4. [c] $\bar{D}_0$ and $\bar{k}_D$ were obtained from quasi-elastic light-scattering measurements.

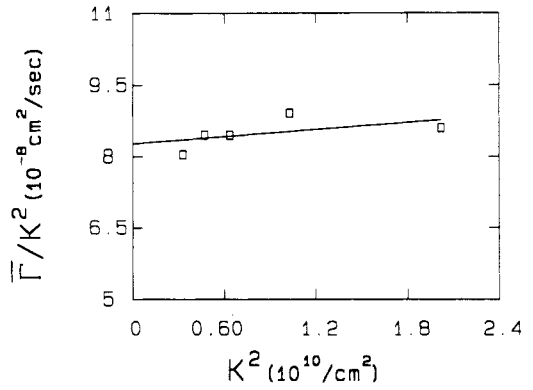

Figure 2. Plot of the K^2-scaled average characteristic line width Γ, $\bar{\Gamma}/K^2$, versus K^2 for sample no. 41 at $C = 3 \times 10^{-4}$ g/mL.

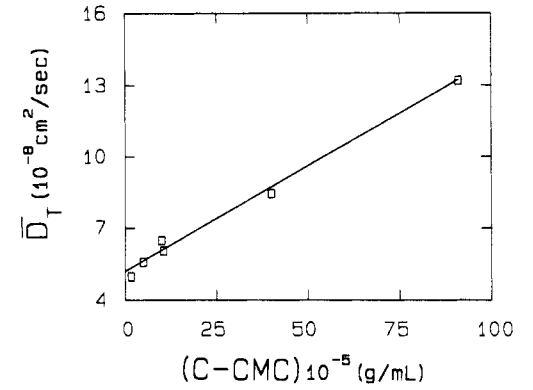

Figure 3. Plot of the average translational diffusion coefficient, $\bar{D}_T$, versus concentration (C − cmc) for sample no. 23.

value of $\bar{\Gamma}/K^2$ represented the z-averaged translational motion of the system. With increasing scattering angle, $P(KR_h)$ of large particles dropped faster than that of small particles. The measured line width would be then weighted more toward small particles, resulting in an increase of $\bar{\Gamma}/K^2$. After angular extrapolation and concentration extrapolation of $\bar{\Gamma}/K^2$ (Figure 3 shows a typical example), the average value of k_D, $\bar{k}_D$, and the average value of D_0, $\bar{D}_0$, could be obtained (Table II). It should be noted that the diffusion second virial coefficient, $\bar{k}_D$, increased when the molecular weight and the size of micelles increased.

3. Size Distribution Analysis. From the results of Laplace inversion of the measured intensity–intensity autocorrelation function, two well-distinguished and narrow peaks were found in line-width distribution for data measured in scattering angles from 25 to 130° (K^2 from 3.3×10^9 to 5.7×10^{10} cm^{-2}). Each peak is a narrow distribution with variance of <0.05. Figures 4 and 5 show a typical distribution of Γ/K^2 and the goodness of the fitting. Since the scattered intensity of micelles is proportional to their mass concentration, molecular weight, and scattering form factor, $P(KR_h)$, such a distribution (Figure 4, solid line) has to be rescaled by the molecular weight and $P(KR_h)$ to obtain a distribution that is weighted by concentration. The dashed line in Figure 4 shows a

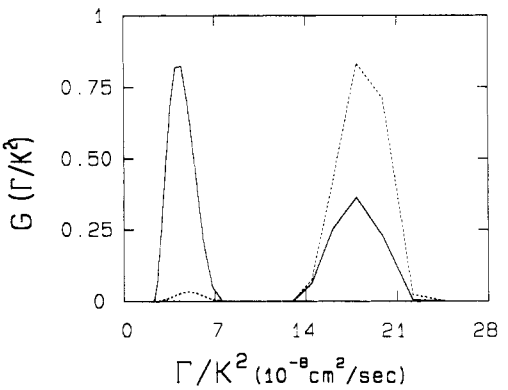

Figure 4. Distributions of the z-weighted (solid line) and weight-weighted (dashed line) translational diffusion coefficient (K^2-scaled characteristic line width) from the Laplace inversion of the autocorrelation function by CONTIN. Sample no. 19 at 25 °C, $C = 2 \times 10^{-4}$ g/mL, and $\theta = 25°$. $D_{T1} = 4.45 \times 10^{-8}$ cm^2 s^{-1}, $Var_1 = 0.04$; $D_{T2} = 17.7 \times 10^{-8}$ cm^2 s^{-1}, $Var_2 = 0.008$; $\bar{D}_T = 10.3 \times 10^{-8}$ cm^2 s^{-1}, Var = 0.42. Var is the variance ($\equiv \int (D_T - D'_T)^2\, dD/D'^2_T$), $D'_T = D_{T1}$ or D_{T2} or $\bar{D}_T$, respectively.

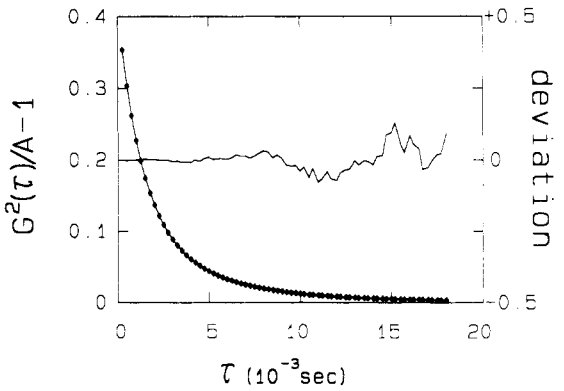

Figure 5. Comparison of the fitted result (line) of the Laplace inversion (Figure 4, solid line) with the original data (diamonds) from sample no. 19 at 25 °C, $C = 2 \times 10^{-4}$ g/mL, and $\theta = 25°$ and the relative fitting deviation.

distribution after such a rescaling. It should be noted that an approximation of $D \propto M^{-1/3}$ has been used in the rescaling. After concentration extrapolation and space conversion (eqs 7 and 8), we were able to obtain two hydrodynamic radii for each sample, which are listed in Table III. The ratio of the two peaks in the line-width distribution indicates their relative population. While the peak positions were relatively stable, the population ratio of the two peaks has an uncertainty of ~15% for measurement performed at various angles. Surprisingly, we found that the population ratio had a strongly reverse concentration dependence, i.e., the higher the concentration, the higher the percentage of the small-micelle component. In solutions of concentrations higher than $\sim 2 \times 10^{-3}$ g/mL for sample no. 23, the large-micelle component disappeared. Figure 6 represents the fraction of the scattered intensity from the small micelles as a function of copolymer concentration. This population variation is the main

Table III
Parameters of PS-PEO Micelles and PS-PEO Aggregated Clusters in Aqueous Solution[a]

sample	R_{h1}, nm	R_{h2}, nm	R_{h1}/ψ, Å	R_{h2}/ψ, Å	W_1	N_1	N_2	r_c, nm	$v_{EO,s}$, Å^3	$V_{EO,l}$, Å^3	zigzag, nm	meander, nm
23	22	70	2.9	9.1	0.87	290	1.0×10^4	11	340	250	144	80
41	19	74	2.8	11	0.96	120	6700	5.6	480	490	162	90
19	12	57	4.6	22	0.97	38	1.2×10^4	3.8	790	220	36.7	20

[a] $\psi \equiv N_A^{3/5}N_B^{4/25}$ for samples 23 and 41 and $\psi \equiv N_A^{3/5}N_B^{4/25}2^{-19/25}$ for sample 19. R_{h1} and R_{h2} are the hydrodynamic radii of the two populations resolved from the Laplace inversion of the photon correlation functions; W_1 is the weight-weighted population percentage of the smaller peak from the same Laplace inversion. N_1 and N_2 are the association numbers of the two populations resolved from eqs 10–13. r_c is the core size of the core–shell micelles from eq 14. $v_{EO,s}$ and $v_{EO,l}$ are the average volumes occupied by water per EO unit in the small micelles and in the large clusters, respectively. Zigzag and meander are the predicted PEO chain lengths according to the zigzag and the meander model, respectively. The values for sample 19 were calculated according to the star model applied to an A–B–A structure.

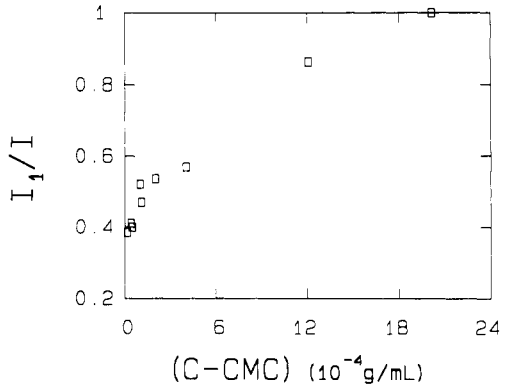

Figure 6. Fraction of the scattered intensity from the small micelles as a function of the copolymer concentration for sample no. 23.

reason for the average diffusion coefficient having a strong concentration dependence as shown in Figure 3.

Recently, according to careful examination of results from dynamic light scattering and from electron microscopy (EM) measurements, several instances have been reported, where amphiphilic micelles exist in two narrowly distributed populations.[3-5] The origins of the paucidisperse distribution were attributed differently by the authors. In an EM study of PS–PEO in water with a copolymer molecular weight of 6.3×10^4 g/mol and 83% (weight) of PEO, Khan et al.[3] attributed the source for the large spherical particle (R_{EM} = 65 nm) as being incomplete dissolution of the bulk copolymer when compared with the small spherical particles of R_{EM} = 5.4 nm, but these large particles could not be removed by heating in various cycles. In the study of association of triblock polycaprolactam–polystyrene–polycaprolactam copolymer in a 50% mixture of toluene–tetrafluoropropanol, Tuzar et al.[4] found that the molecular weight ratio of the large hemispherical particles to the small ones was 70 from EM measurement; the apparent average molecular weight obtained through dynamic light scattering was close to that of the large particles. The authors speculated that the formation of the large particle was from the coalescence of small micelles due to the selective sorption of tetrafluoropropanol on the surface of micelles. On the other hand, Brown and his co-workers[5] attributed to slow motion from dynamic light-scattering measurement of Triton X-100 [[*p*-(1,1,3,3-tetramethylbutyl)phenyl]poly(oxyethylene)] in aqueous solution to loose clusters of the smaller micelles, which might be the precursor stage of the liquid-crystalline phase.

In the present study, we also observe two populations, stable in time. We attribute the smaller particles to normal spherical core–shell micelles. The nature of the larger aggregates is still unclear. We envision several possibilities, (1) a single large core–shell micelle, (2) an onionlike particle with alternating concentric layers of solvated and undissolved blocks, or (3) a loose cluster of small regular micelles. The multilayer structure would be more favored by ABA triblock copolymers than diblock copolymers,[28] yet large aggregates are observed here for both types of copolymers. Furthermore, if the polystyrene phases are indeed glassy, reorganization of the smaller micelles to larger core–shell or multilayer aggregates upon dilution in water at 22 °C might be expected to be very slow. Indeed, this unique finding that the fraction of large aggregates increases upon diluting the sample suggests to us that the origin of particle aggregation is related to the behavior of PEO in aqueous solution.

PEO has some remarkable properties when dissolved in water. It readily dissolves in water, but, like many water-soluble polymers, it has a lower critical solution temperature (LCST ~ 100 °C).[22,29] Many studies have shown that, even at room temperature, aqueous solutions of PEO can form large and loose thermodynamically reversible association complexes coexisting with another type of aggregate. Some of the complexities are demonstrated in the recent work of Polik and Burchard.[22] The forces leading to clustering of PEO molecules in water could involve hydrogen bonding, the structure of water, and the hydrophobic effect. It is therefore not that surprising that in water PEO–PS micelles with long PEO chains as an outside layer have a tendency to form aggregates (or association complexes) depending on the copolymer composition and the solution condition.

Some further insights into the micelle structure and that of the larger aggregates can be gained by comparing our results with theory. According to the star model proposed by Halperin[9] for a core–shell particle formed from an AB diblock copolymer in the case of $N_A \gg N_B$, the radius of a particle is

$$R \propto N_A^{3/5}N_B^{4/25}a \tag{9}$$

with a being a typical monomer size. The ratio of our measured R_h values to $N_A^{3/5}N_B^{4/25}$ should be a constant for the two diblock copolymer samples. From Table III the ratio $R_h/N_A^{3/5}N_B^{4/25}$ is the same for the two small particles of diblock copolymer samples. No such equality holds for the large particles, which excludes the possibility of the core–shell structure for these aggregates.

From the weak angular dependence of the two characteristic line widths resolved from the autocorrelation function, it is reasonable to assume that both populations are spherical. If we assume that the small particles are core–shell micelles and the large ones are due to an association of micelles, the following procedure can yield the dimensions and the particle weights for both populations from the measured values based on the star model.[9]

In the star model, when the solvent compatible block length is larger than that of the incompatible block ($N_A \gg N_B$), the association number (N_1) for a micelle is

proportional to $N_B^{4/5}$. For the aggregated cluster, we can, as a first approximation, scale the particle weight to the cube of its radius (R_{h2}) and its density. Thus, the molecular weights of the micelles (M_1) and the aggregated cluster (M_2) can be computed according to the following equations:

$$M_w = W_1M_1 + (1 - W_1)M_2 \tag{10}$$

$$\frac{M_{1,s1}}{M_{1,s2}} = \frac{M_{n,s1}}{M_{n,s2}}\left(\frac{N_{B,s1}}{N_{B,s2}}\right)^{4/5} \tag{11}$$

$$\frac{M_{2,s1}}{M_{2,s2}} = \frac{\rho_{s1}}{\rho_{s2}}\left(\frac{R_{h2,s1}}{R_{h2,s2}}\right)^3 \tag{12}$$

The subscripts s1 and s2 in eqs 11 and 12 denote sample 1 and sample 2, respectively. The density of the micelle cluster is expected to be proportional to the density of its constituents, the overall density of a single micelle, which can be scaled as

$$\rho = \frac{M_1}{V} \propto \frac{M_nN_1}{R^3} \propto \frac{M_nN_B^{4/5}}{N_A^{9/5}N_B^{12/25}} = M_nN_A^{-9/5}N_B^{8/25} \tag{13}$$

In eq 13 M_n is the copolymer molecular weight. By substitution of the measured M_w, W_1, and R_{h2} of the samples no. 23 and no. 41 into eqs 10–13, the particle weight for both populations of the two samples can be computed. The results are listed in Table III. We have used the proportionality constant from the diblock copolymers combined with the values from the triblock copolymer (sample no. 19) to obtain the particle weight of no. 19. Again, we have found the same trend; i.e., the association degree of the micelles increases by increasing the copolymer molecular weight or by decreasing the PEO content, for the association number (N_1) as in the average value (N).

If we accept the assumption that the "insoluble" core (PS) has the same density as bulk PS,[30] the core volume V_c can be related to the association number, N_1, and the volume of each individual PS chain V_{ps}

$$V_c = \frac{4\pi r_c^3}{3} = V_{ps}N_1 = \frac{M_nW_BN_1}{\rho_{PS}N_A} \tag{14}$$

In eq 14 W_B is the weight percentage of PS in the copolymer sample. The r_c values calculated are listed in Table III.

From the shell thickness ($R_{h1} - r_c$), the mean volume occupied by water per EO unit in the shell ($V_{EO,s}$) could be calculated, and these values are listed in Table III. From the molecular volumes of 64.6 Å^3 for one EO unit and 30 Å^3 for one water molecule, the average numbers of water molecules per EO unit can be estimated. These values indicate that the PEO chains in the shell are highly swollen: the PEO coils have trapped large amounts of water in addition to these involved in hydrogen bond formation between the ether oxygens and water (i.e., two water molecules per EO unit[32]). The degree of hydration increases with increasing PEO chain length, a result known for micelles composed of low molecular weight PEO derivatives ($N_A \sim 10$–20).[32] It has also been found that the trapped water per EO unit is temperature dependent.[25] It would be interesting in future studies to see if $v_{EO,s}$ varies in a similar manner as a function of temperature.

From the data in Table III we see that for diblock copolymers the magnitude of $v_{EO,s}$ increases with increasing shell thickness and with increasing PEO chain length, i.e., the closer to the core, the more compact the PEO chains. This makes sense since there is less space for the water molecules near the core surface than further outside; the proportion of water molecules per EO unit then increases as the shell thickness increases. This could be one of the main reasons we were unable to fit our results to theories (for example, the model in ref 31), in which a uniform copolymer segment concentration in the shell was assumed.

To calculate the volume of water occupied per EO unit in the large micelle clusters, we have to subtract from the total hydrodynamic volume of the cluster, the volume occupied by the polystyrene in the micelle core (161.2 Å^3 per styrene unit[10]) and by the PEO units in the swollen shell, and divide this difference by the numbers of EO units in the cluster. Thus, the average volume occupied by water per EO unit can be estimated as

$$v_{EO,l} = \frac{\frac{4\pi}{3}R_{h2}^3 - N_2(64.6N_A + 161N_B)}{N_2N_A} \tag{15}$$

These $v_{EO,l}$ values as listed in Table III are remarkably close to that of regular micelles ($v_{EO,s}$). This further confirms that the structure of the large component is a loose cluster of regular micelles.

Generally, there are two extreme configurations for an elongated PEO chain. One is the "zigzag" model, in which the chain is fully extended with the length and width of each EO unit amounting to 3.6 and 2.5 Å, respectively. The other is the "meander" model, in which the chain is twisted into an expanded helical coil form with the length and width being 2.0 and 4.5 Å, respectively.[33] The results of the chain lengths calculated according to these two models are listed in Table III. Comparison of the thickness of the shell ($R_{h1} - r_c$) in the PEO–PS micelles with these calculated end-to-end distances indicates that the PEO chain is not fully elongated in protruding from the core.

Conclusions

PEO–PS diblock and triblock copolymers form spherical micelles in aqueous solution. Determination of the molecular weight, aggregation number, and the hydrodynamic radius of each micelle is complicated by the tendency of the micelles to aggregate into loose clusters. These are best observed in terms of a sharp bimodal size distribution in dynamic light-scattering experiments. Due to the bimodal distribution, neither the micelle dimensions nor the association numbers can be deduced from measurements that give only ensemble averages. Since the weighting between micelles and micellar clusters may vary, depending on the experimental conditions, the resulting average micelle weight can appear to change from one experimental method to another. The sizes of both core–shell micelles and micellar clusters are insensitive to changes in concentration, and both are spherical in shape. With an appropriate Laplace inversion algorithm applied to the autocorrelation function, information about the micelle association number can be easily retrieved with a commercial particle sizer. However, a unique interpretation of the finding that W_1 is concentration dependent is still to be elucidated.

Acknowledgment. We thank Professor Benjamin Chu for the use of his laboratory in performing part of the light-scattering measurement and Professor G. Vancso for the use of the refractometer. This research is supported by the NSERC (Canada) through its Operating and University–Industry Programmes and the Province of Ontario through its URIF fund.

References and Notes

(1) Tuzar, Z.; Kratochvil, P. *Adv. Colloid Interface Sci.* **1976**, *6*, 201.

(2) Emmelius, M.; Hoerpel, G.; Ringsdorf, H.; Schmidt, B. In *Polymer Science and Technology*; Chiellini, E., Giusti, P., Migliaresi, C., Nicolais, L., Eds.; Plenum: New York, 1986; Vol. 34, p 313.
(3) Khan, T. N.; Mobbs, R. H.; Price, C.; Quintana, J. R.; Stubbersfield, R. B. *Eur. Polym. J.* **1987**, *23* (3), 191.
(4) Tuzar, Z.; Stehlicek, J.; Konak, C.; Lednicky, F. *Makromol. Chem.* **1988**, *189*, 221.
(5) Brown, W.; Rymden, R.; Stam, J.; Almgren, M.; Svensk, G. *J. Phys. Chem.* **1989**, *93*, 2512.
(6) de Gennes, P.-G. In *Solid State Physics*; Liebert, J. Ed.; Academic: New York, 1978; supplement 14, p 1.
(7) Leibler, L.; Orland, H.; Wheeler, J. C. *J. Chem. Phys.* **1983**, *79*, 3550.
(8) Noolandi, J.; Hong, M. H. *Macromolecules* **1983**, *16*, 1443.
(9) Halperin, A. *Macromolecules* **1987**, *20*, 2943.
(10) Nagarajan, R.; Ganesh, K. *J. Chem. Phys.* **1989**, *90*, 5843.
(11) Whitmore, M. D.; Noolandi, J. *Macromolecules* **1985**, *18*, 657.
(12) Munch, M. R.; Gast, A. P. *Macromolecules* **1988**, *21*, 1360.
(13) Riess, G.; Rogez, D. *Polym. Prepn. (Am. Chem. Soc., Div. Polym. Chem.)* **1982**, *23*, 19.
(14) Bahadur, P.; Sastry, N. V.; Rao, Y. K.; Riess, G. *Colloid Surf.* **1988**, *29*, 343.
(15) Nakamura, K.; Endo, R.; Takeda, M. *J. Polym. Sci., Polym. Phys. Ed.* **1976**, *14*, 135 and 1287.
(16) Zhao, C.; Winnik, M. A. *Langmuir* **1990**, *6*, 514.
(17) Wilhelm, M.; Zhao, C.; Wang, Y.; Xu, R.; Winnik, M.; Mura, J.; Riess, G.; Croucher, M. *Macromolecules*, in press.
(18) We draw the readers attention to very interesting recent work on PS–PEO block copolymer micelle formation in aliphatic hydrocarbon solvents: Cogan, K. A.; Gast, A. P. *Macromolecules* **1990**, *23*, 745.
(19) Munch, M. R.; Gast, A. P. *Macromolecules* **1990**, *23*, 2313.
(20) Marti, S.; Nervo, J.; Riess, G. *Prog. Colloid Polym. Sci.* **1975**, *58*, 114.
(21) Riess, G.; Nervo, J.; Rogez, D. *Polym. Eng. Sci.* **1977**, *17*, 634.
(22) Polik, W. F.; Burchard, W. *Macromolecules* **1983**, *16*, 978.
(23) Alfrey, T., Jr.; Bradford, E. B.; Vanderhoff, J. W. *J. Opt. Soc. Am.* **1964**, *44*, 603.
(24) Hallett, F. R.; Craig, T.; Marsh, J.; Nickel, B. *Can. J. Spectrosc.* **1989**, *34*, 63.
(25) Zhou, Z.; Chu, B. *J. Colloid Interface Sci.* **1988**, *126*, 171.
(26) Benoit, H.; Froelich, D. In *Light Scattering from Polymer Solution*; Huglin, M., Ed.; Academic Press: London, 1972; Chapter 11.
(27) Software for the NNLS fitting were provided (in part) by Brookhaven Instrument, Inc., and for the CONTIN fitting were provided by S. W. Provencher.
(28) Beamish, A.; Goldberg, R. A.; Hourston, D. J. *Polymer* **1977**, *18*, 49.
(29) Rowlinson, J. S. *Liquid and liquid mixtures*, 2nd ed.; Butterworths: London, 1969; p 167.
(30) Fluorescent probe studies[16,17] support this point of view, but further evidence is needed.
(31) Alexander, S. *J. Phys. (Paris)* **1977**, *38*, 983.
(32) Elworthy, P. H.; Macfarlane, C. B. *J. Chem. Soc.* **1964**, 311.
(33) Rosch, H. In *Nonionic Surfactants*, Schick, M. J., Ed.; Dekker: New York, 1967.

Registry No. (Styrene)(ethylene oxide) (block copolymer), 107311-90-0.